Journal of
Ceramic Science
and Technology

J. Ceram. Sci. Tech., **08** [01] 113-120 (2017)
DOI: 10.4416/JCST2016-00095
available online at: http://www.ceramic-science.com

Development of Damage-Tolerant Ceramic Matrix Composites (SiC/SiC) using Si-BN/SiC/pyC Fiber Coatings and LSI Processing

B. Mainzer*[1], R. Jemmali[1], P. Watermeyer[2], K. Kelm[2], M. Frieß[1], D. Koch[1]

[1]Institute of Structures and Design, German Aerospace Center (DLR),
Pfaffenwaldring 38 – 40, D-70569 Stuttgart, Germany
[2]Institute of Materials Research, German Aerospace Center
(DLR) Linder Höhe, D-51147 Cologne, Germany

received October 31, 2016; received in revised form January 6, 2017; accepted January 27, 2017

Abstract

Silicon-carbide-fiber-reinforced silicon carbide matrix composites (SiC/SiC) exhibit good thermal shock resistance, a low coefficient of thermal expansion and excellent physical properties as well as chemical stability at elevated temperatures and are therefore regarded as promising candidates for various applications in heavily loaded turbine sections of jet engines. Liquid silicon infiltration was chosen as a technique characterized by short processing times to obtain composites with low porosity in a three-step process: infiltration of fiber preforms with a phenolic resin, pyrolysis and siliconization. Unfortunately, uncoated Tyranno SA3 fibers were cramped in the matrix, resulting in SiC/SiC with low strength and damage tolerance. In order to protect the fibers and to simultaneously provide a weak fiber matrix bonding, a CVD Si-BN/SiC/pyC fiber coating was chosen. The triple coating leads to a twofold higher bending strength of SiC/SiC as well as to more damage-tolerant fracture behavior compared to composites without fiber coating. Composites with various fiber volume contents are compared with regard to their mechanical properties. The microstructure of the composites was characterized by means of scanning electron microscopy (SEM), transmission electron microscopy (TEM) and computed tomography (CT), especially with regard to the functionality of the fiber coating.

Keywords: SiC/SiC, liquid silicon infiltration, Tyranno SA3, fiber coating

I. Introduction

(1) Silicon-carbide-fiber-reinforced silicon carbide

A ceramic-fiber-reinforced composite that has recently found its way into application in jet engines is silicon-carbide-fiber-reinforced silicon carbide (SiC/SiC) [1]. Besides high resistance against oxidation and high thermal conductivity, the thermal shock resistance allows operating temperatures over 1200 °C under cyclic thermal loads. Therefore, SiC/SiC composites are a lightweight alternative for the nickel-based superalloys currently used in the hot sections of jet engines. A higher temperature capability allows reduced cooling air consumption and thereby improved fuel efficiency and reduced emissions.

A variety of methods is available to manufacture non-oxide ceramic matrix composites, which can be distinguished by the way the matrix is created. The most important techniques are chemical vapor infiltration (CVI), polymer infiltration and pyrolysis (PIP) as well as reactive melt infiltration (RMI) [2].

This work focuses on obtaining SiC-fiber-reinforced composites with the liquid silicon infiltration process (Fig. 1). This process, also known as LSI, is a special type of reactive melt infiltration method. It is a three-stage process, beginning with the infiltration of a SiC fiber-preform with a matrix precursor. After the infiltration and curing, this step is followed by pyrolysis and silicon infiltration. One of the most prominent examples of a LSI-SiC/SiC is the Hipercomp material developed by General Electric which has been used since 2016 in the LEAP jet engine for turbine shrouds [3]. This material is based on CVD-coated Hi-Nicalon or Hi-Nicalon Type S fibers and a particle-based matrix. The fiber coatings consist of BN and an overcoating of Si_3N_4 or SiC. BN is used for damage tolerance, Si_3N_4 and SiC are used as a barrier against silicon. As matrix precursor either a SiC slurry or a SiC- and C-particle-loaded polymer is used. After pyrolysis, the fibrous preform is infiltrated with silicon. Others have also tried the SiC slurry approach in combination with pyC/SiC-coated Nicalon fibers and BN/SiC-coated Hi-Nicalon and Sylramic fibers [4–5]. Aoki *et al.* used a mixture of carbon black with a polyurethane resin as matrix precursor and a silicon-hafnium alloy to reduce the melting point of silicon and therefore to reduce the thermal degradation of SiC fibers during processing [6]. In that work, a pyC/SiC CVD-coating was used on Tyranno ZMI fibers.

In the present study, SiC/SiC composites are manufactured by means of a new approach using a pure polymer

* Corresponding author: bernd.mainzer@dlr.de

precursor that is pyrolyzed to generate a porous carbon matrix. Thanks to a low-viscous polymer, homogeneous infiltration is possible, circumventing sieving effects compared to particle-based systems. Resin transfer molding enables homogeneous infiltration of the fiber bundles by the resins as well as control of the temperature and pressure during the curing process. Nevertheless, the application of pure polymers requires mechanisms that lead to the formation of a carbon matrix with high porosity. The microporous matrix can be used to obtain homogeneous infiltration and good conversion of silicon to SiC.

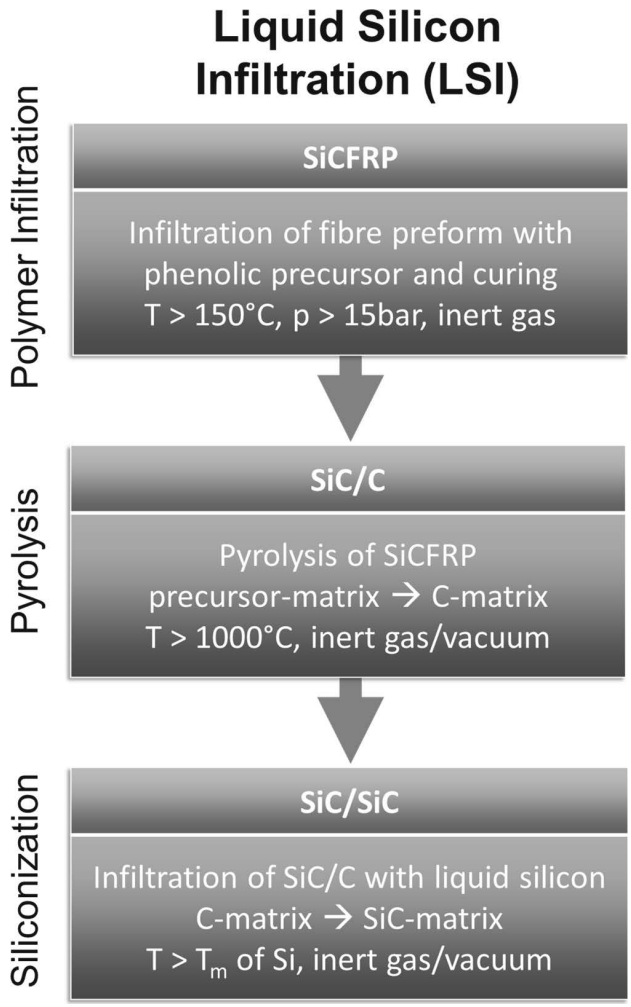

Fig. 1: Scheme of the LSI process.

(2) Role of the fiber coating

Monolithic ceramics exhibit brittle failure when mechanically loaded. In order to overcome this characteristic, reinforcing fibers can be embedded into the brittle matrix. Although the fibers often exhibit brittle behavior too, a non-brittle, damage-tolerant SiC/SiC composite can be achieved by creating a Weak Interface Composite (WIC). During crack propagation, this concept provides high damage tolerance based on energy-dissipating effects such as fiber pullout, crack branching or crack deflection [7–8].

Typically weak interfaces in composites can be achieved with pyrolytic carbon (pyC) or boron nitride fiber coatings. Nevertheless, the suitability of both of these coatings is limited in LSI composites. PyC easily reacts with liquid silicon to silicon carbide and boron nitride prevents good infiltration owing to high contact angles against silicon [9].

In previous research, a double-fiber coating of BNx/SiNx was investigated in combination with a resole-type phenolic resin. It was observed, that the NaOH in the resin attacked the BN layer [10]. In addition, a favored foam-like carbon microstructure was not achieved on this particular type of coating. In the present work, a two-layered fiber coating was applied, consisting of a silicon-doped boron nitride and SiC and compared to a three-layered coating with an additional pyC layer. The Si-BN functions as a weak interface with improved oxidation resistance, SiC is a reaction barrier against silicon. PyC is intended to provide good wetting and bonding with the carbon precursor as well as to enable the formation of the desired, easily convertible carbon foam (Fig. 2). In order to prevent decomposition of the Si-BN layer, a NaOH-free novolac-type phenolic resin was applied.

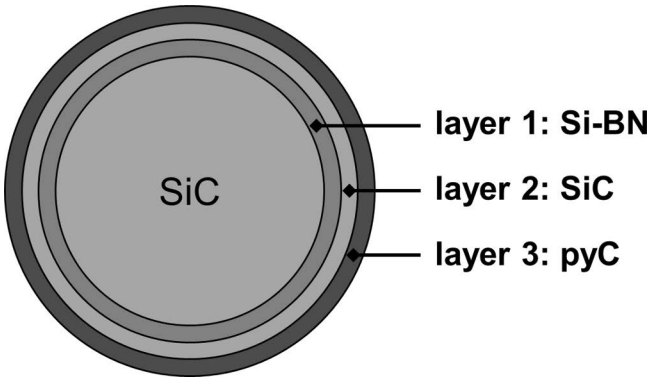

Fig. 2: Scheme showing the concept of the three-layered fiber coating with Si-BN/SiC/pyC.

II. Experimental Procedure

(1) Manufacturing of the composites

A total of three SiC/SiC plates were manufactured with dimensions of 80 x 40 x3 mm^3 consisting of Tyranno SA3 plain weave fabrics with an area weight of 260 g/m^2 in order to investigate the influence of the fiber coating on mechanical properties. The fiber coatings were applied by means of chemical vapor deposition. The Si-BN layer was produced from BCl_3 and NH_3 with an added chlorosilane for the Si dopant. The SiC layer was produced from $HSiCl_3$ and H_2 and the pyC was produced from a hydrocarbon source. All processes were performed under vacuum at a process pressure < 20 mbar and with temperatures in the range of 900 – 1100 °C (Archer Technicoat Ltd, United Kingdom). One plate was manufactured with a fiber volume content of 36 % and a three-layered coating consisting of Si-BN/SiC/pyC (Fig. 3). This composite is hereinafter referred to as Type 1 composite. In order to gauge the functionality of the coating, one plate was manufactured using only 18 % of coated fibers, which was half of the amount in comparison to the first plate. An additional 22 % uncoated fibers were stacked in between every coated layer, creating a laminate (Type 2). As a reference, a plate with a fiber volume content of 40 % uncoated fibers was

manufactured as well (Type 3). A fourth composite was manufactured with a double coating consisting of Si-BN and SiC and a fiber volume content of 36 % (Type 4).

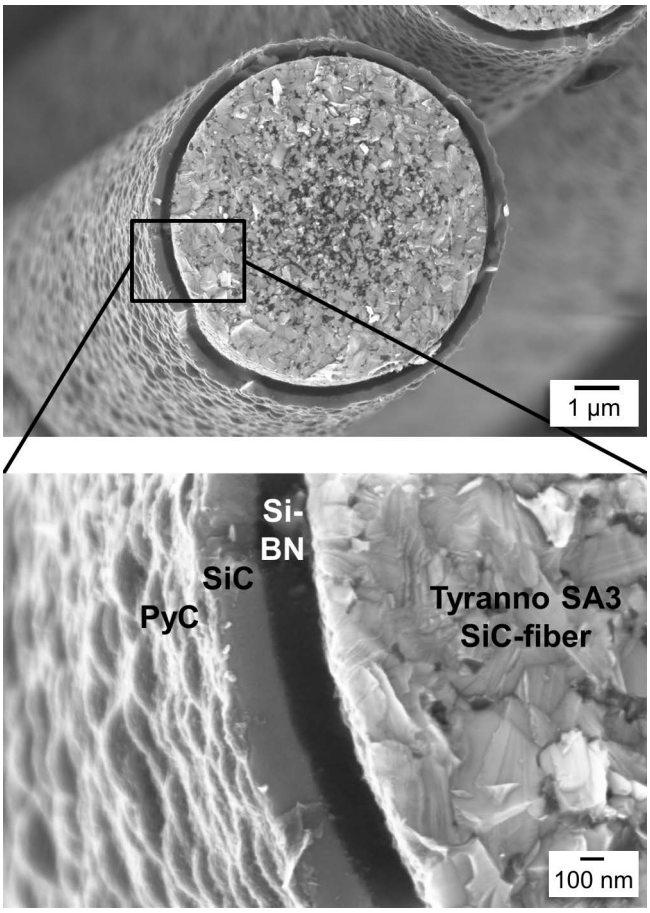

Fig. 3: SEM images of cross-sections of the Si-BN/SiC/pyC coating on a Tyranno SA3 fiber.

Fibers without coating were thermally desized at 600 °C in argon atmosphere at a pressure of 1 bar. The fabrics were laid on top of one another and inserted into a mold. The desired fiber volume content of each plate was defined by the spacers. A novolac-type phenolic carbon precursor (Hexion GmbH, Germany) was infiltrated at 80 °C by means of resin transfer molding. After the plates had been fully infiltrated, the curing process was realized at 150 °C in a nitrogen atmosphere with a pressure of 20 bar. The composites were subsequently pyrolyzed in vacuum at 1400 °C to convert the polymer matrix into a carbon matrix. In a separate step, an excess of a molten silicon-boron alloy with 8 at% boron (eutectic composition) was used for the infiltration into the porous SiC/C preform to convert the carbon matrix to silicon carbide. The boron allowed gentle, low-temperature siliconization at 1400 °C. After processing, the surfaces were slightly ground to get rid of excess silicon.

(2) Characterization of the composites

For a more detailed investigation of the RMI process, a small sample with dimensions of 40 x 10 x 3 mm^3 of the Type 1 composite was prepared for µCT. After each of the three steps of the LSI process, the sample was scanned at exactly the same position. The scans were performed using a high-resolution µCT-System (nanotom, GE Sensing & Inspection Technologies GmbH, Germany) consisting of a nanofocus X-ray tube with a maximum voltage of 180 kV and a 12-bit flat panel detector with an active area of 2348 x 2348 pixels at 50 microns per pixel. The µCT scans were performed with the X-ray parameters 80 kV/180 µA at an exposure time of 1000 ms. The acquired X-ray images were reconstructed with a special algorithm known as Filtered Back Projection.

In order to determine the bending strength of the composites, a total of four samples each with dimensions of 36x10x3 mm^3 with ground surfaces were prepared. The samples were tested in a 3-point bending test with a support distance of 30 mm. Their Young's modulus was determined with strain gauges.

SEM images were taken from polished cross-sections of fibers and composites with an In-Lens (SE1 secondary electron) detector. Images of fractured surfaces were taken with the SE detector (SE2 secondary electron detector, Everhart-Thornley type). For both imaging modes, an acceleration voltage of 5 kV was chosen (Zeiss Ultra Plus, Carl Zeiss Microscopy GmbH, Germany).

Transmission electron microscopy (TEM) investigations were performed on focused ion beam (FIB) prepared lamellae of the Type 1 composite. FIB sections were obtained with a dual-beam FEI Helios 600i FIB-SEM system equipped with a FEI micro manipulator (FEI, Hillsboro, USA). After electron- and ion-beam coating with platinum, trench cutting with 30 keV Ga+ ions was followed by lift-out. The lamellae were then mounted on Omniprobe lift-out grids (Omniprobe Inc., Dallas, USA) and thinned with successively reduced ion beam currents. For a final polishing step, the acceleration voltage was reduced from 30 kV to 5 kV.

TEM investigations were conducted by means of a Philips Tecnai F30, 300 keV, field emission transmission electron microscope, equipped with a "Super-Twin" objective lens. Furthermore, the system is equipped with a bottom-mounted CCD camera (Gatan MSC 749) and a Gatan imaging filter (GIF 2002, Gatan Inc., Pleasanton, USA).

III. Results and Discussion

(1) Investigation of the RMI process

The µCT setup was used to monitor the microstructural changes in the Type 1 composite after each step in the RMI process. After resin transfer molding, the composite was non-porous (Fig. 4a). Although the selected spot is rather small in comparison to the composite, this density is typical for composites manufactured with the resin transfer molding technique. During pyrolysis the polymer matrix was converted to a carbon matrix. This conversion is associated with shrinkage owing to the emission of volatile compounds in combination with an increase in density. However, because of the reinforcing fibers, global shrinkage of the composite is suppressed. Outside of the fiber bundles, the evolution of carbon blocks and large voids

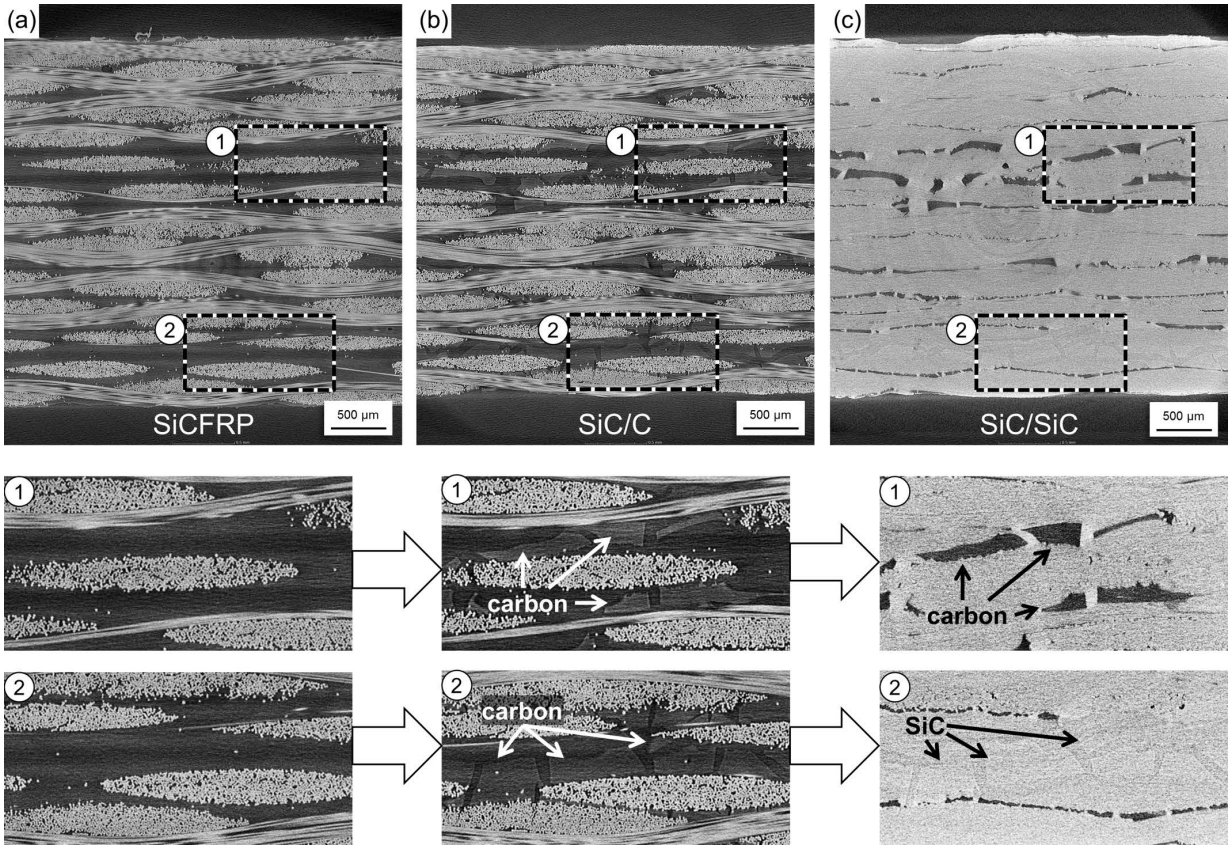

Fig. 4: µCT cross-sections of the same slice in the Type 1 composite. Two spots are enlarged in each cross-section for better visualization of the evolution of carbon and porosity and conversion to SiC: (a) fully dense composite after RTM process; (b) evolution of carbon blocks and porosity outside of fiber bundles; (c) fully dense composite after silicon infiltration, some carbon blocks remain unconverted, some blocks are converted to SiC.

was observed (Fig. 4b). After silicon infiltration, the composite was fully dense again. Some of the carbon blocks were converted to SiC while others remained largely unconverted (Fig. 4c).

To investigate this behavior in more detail, SEM images of the pyrolyzed and siliconized state were captured. The pyrolyzed sample was prepared so as to obtain a clear view of the porous carbon microstructure (Fig. 5a). Within the fiber bundles, the carbon showed good adherence to the fiber surface. Besides the already seen large voids outside of the fiber bundles, the carbon exhibited very fine porosity as well. The size and amount of pores was highly dependent on the position inside the composite. Within the fiber bundles, the carbon showed a highly open porous foam-like microstructure with pores with diameters of up to 100 nm (Fig. 5b). In contrast, outside of fiber bundles, much smaller pores below 50 nm in diameter were observed (Fig. 5c).

As already seen in CT images, some carbon blocks in the sample with the Si-BN/SiC/pyC coating were not or just partly converted to SiC during siliconization (Fig. 6a). The siliconized sample was investigated with SEM as well. Within fiber bundles, a complete conversion of carbon was reached while on the outside residual carbon blocks were found. For further investigation of this behavior, EDX analyses of the SiC matrix were performed within the fiber bundles (Fig. 6b) and close to a conversion front inside a carbon block (Fig. 6c). However, EDX on carbon compounds can be prone to errors. In order to verify the accuracy of the detector, the dense outer region of the near stoichiometric Tyranno SA3 fiber was investigated as well. The results are shown in Table 1. Within the fiber bundles, a homogeneous nano-sized silicon-rich silicon carbide microstructure was observed. Outside the bundle in a partly converted block, the SiC matrix was near stoichiometric (Table 1). This can be ascribed to the observed porosity in the pyrolyzed state. The carbon foam within the bundles provides a low amount of carbon to be converted to SiC, while in carbon blocks outside of fiber bundles the porosity might be too low for good infiltration and conversion. This might be due to closed porosity and the distances between the pores being too large with the result that silicon cannot open the next pore. As observed, the surface of the carbon blocks was presumably even denser than the inside, resulting in a 200-nm-thin interface of SiC and no further penetration of silicon into the carbon.

Table 1: EDX results of selected spots in the Type 1 composite (Fig. 6).

EDX spot	Si [at%]	C [at%]	O [at%]
#1	48.9	50.8	0.3
#2	72.2	27.5	0.3
#3	51.7	48.2	0.1
#4	0	98.8	1.2
#5	95.6	3.9	0.5

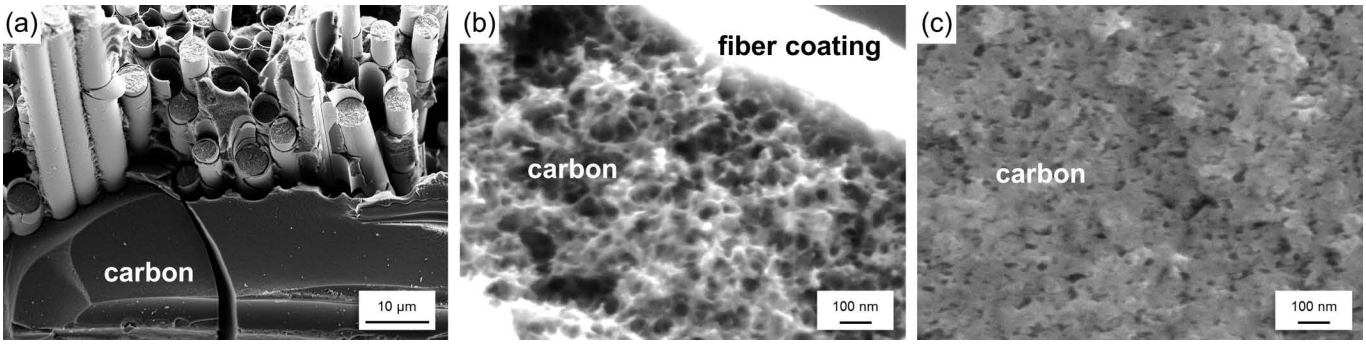

Fig. 5: Microstructure of a fractured surface of the Type 1 composite after pyrolysis: (a) Fiber bundle with attaching carbon block; (b) Porous carbon foam between single filaments, dark spots are pores; (c) Low porosity in carbon outside of fiber bundles.

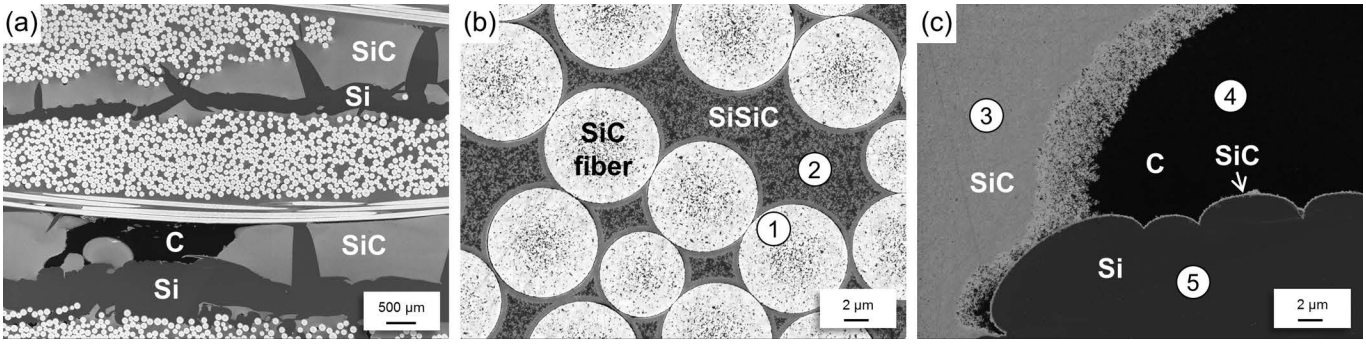

Fig. 6: Polished cross-sections of the composite after silicon infiltration, numbers indicate selected spots for EDX analysis (Table 1): (a) Overview showing coated fibers within a matrix consisting of SiC, Si and unconverted carbon blocks; (b) Evolution of a silicon-rich SiC matrix within fiber bundles; (c) Conversion front at a tri-border area of silicon, carbon and silicon carbide.

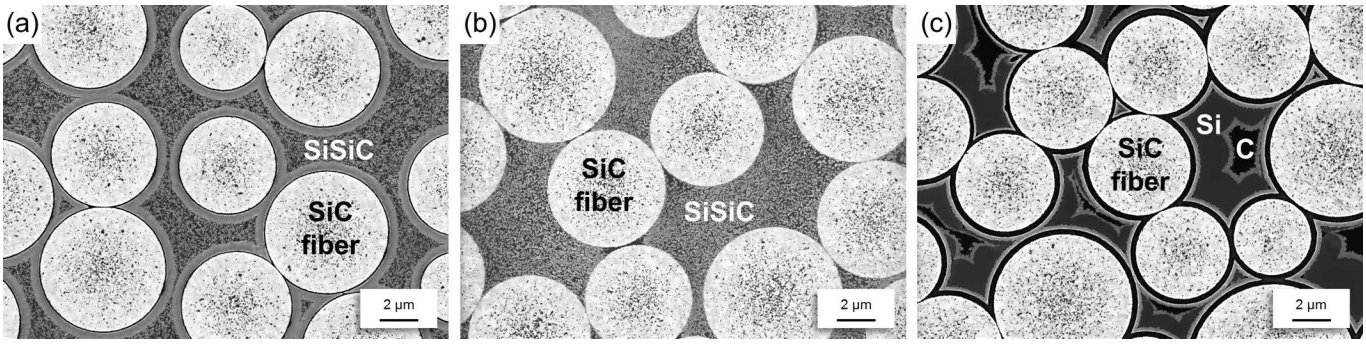

Fig. 7: SEM images of polished cross-sections of SiC/SiC composites: (a) Type 1 composite with Si-BN/SiC/pyC fiber coating; (b) Type 3 composite without fiber coating; (c) Type 4 composite with Si-BN/SiC fiber coating.

(2) The fiber/matrix interface

In SiC/SiC composites manufactured by means of RMI, the fibers and matrix have similar toughness. Hence to provide damage tolerance, a weak interface is mandatory. Depending on the fiber surface, different matrix compositions can be achieved. As already seen in Section III(1), a homogeneous nano-sized silicon-rich silicon carbide matrix was created inside Si-BN/SiC/pyC-coated fiber bundles (Fig. 7a). This is due to the evolution of a carbon foam during pyrolysis, as already seen. The same matrix is created in case of the desized, uncoated fibers (Fig. 7b). Here as well, a carbon foam did occur within the fiber bundles which was easily converted by the melt. Surprisingly, in the case of the double coating of Si-BN/SiC, the precursor did not evolve a carbon foam (Fig. 7c). As a result of the shrinkage during pyrolysis, carbon blocks were created which were small and difficult to convert. Presumably, this behavior is due to selective bonding behavior of the carbon precursor on surfaces. A carbon surface such as pyC or the carbon residue on the thermally desized fibers seems to promote such a strong attachment that the precursor is forced to compensate for the shrinkage by the creation of a foam. In contrast to this, the pure CVD-SiC coating did not provide a good attachment. Similar behavior was observed in previous research on BNx/SiNx-coated Tyranno SA3 fibers with the use of a resole-type phenolic resin [9]. On uncoated fibers, the resin showed a strong bonding and evolved porosity, while on coated fibers the resin created carbon blocks. The results suggest that the formation of porosity is highly dependent on the fiber surface but can easily be influenced by the application of a thin pyC layer.

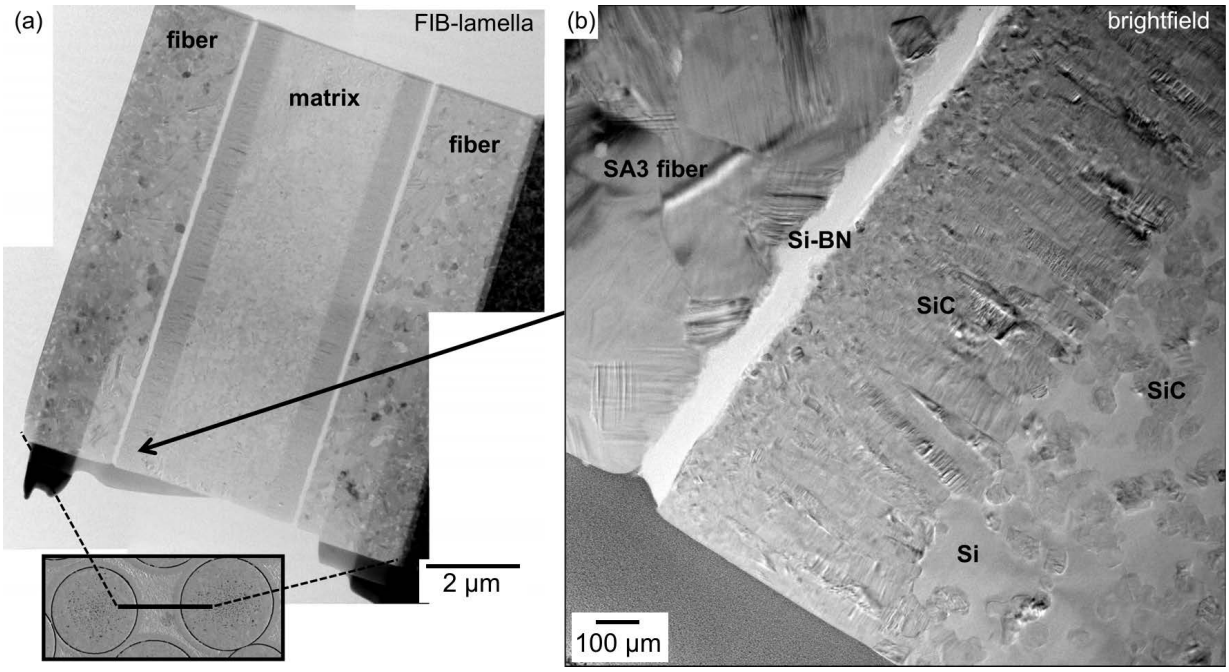

Fig. 8: TEM investigations on a FIB lamella taken from the Type 1 composite utilizing the three-layered fiber coating: (a) the FIB lamella was taken out from between two SiC filaments; (b) image showing the interface fiber/coating/matrix.

Independent of this behavior, after siliconization neither degradation of the fibers nor of the fiber coatings was observed with SEM. The infiltration of the melt into fiber bundles went smoothly with the other three composites. The matrix was crack-free and showed good adherence to the fiber and coating, respectively.

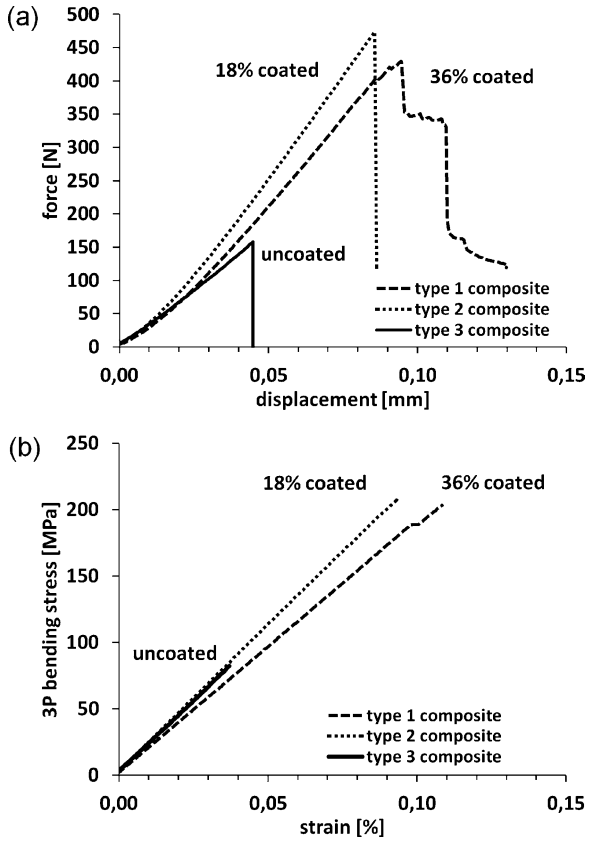

Fig. 9: Representative curves SiC/SiC samples that underwent the 3-point bending test: (a) force/displacement curves; (b) stress/strain curves.

The composite with the Si-BN/SiC/pyC coating was examined with TEM in order to investigate the suitability of the fiber coating with regards to the harsh processing conditions. A lamella was prepared by means of FIB between two coated fibers (Fig. 8a). A closer look at the interface is shown in Fig. 8b. The investigated Si-BN and SiC layers had a thickness of 100 and 800 nm respectively. The pyC layer was not observed any more, presumably it had been converted to SiC. The Si-BN was amorphous in comparison to the crystalline lamellar SiC layer. The silicon-rich matrix contained nano-sized SiC crystals. During processing, the SiC layer stayed intact. Hence, the Si-BN layer was protected from dissolution. All layers of the interface were homogeneous and showed crack-free, good attachment to the fiber and the matrix.

(3) Mechanical properties

A total of four samples each of the manufactured Type 1 – 3 plates were tested in a three-point bending test. The Type 4 composite was not tested owing to its strong delamination during processing. All samples failed on the tensile-loaded side. The Type 1 composite exhibited an average strength of 202 ± 18 MPa. After the maximum stress had been reached, no catastrophic failure occurred, which indicated improved fracture toughness. In comparison, the laminate (Type 2) exhibited an average bending strength of 197 ± 10 MPa. Figs. 9a and 9b show representative stress/displacement and stress/strain curves for both composites.

Although only half of the fabrics were coated, the results were similar to the composite which entirely utilized coated fibers. This behavior may be due to the 3PB test method. The tensile-loaded outer layer of coated fibers carried most of the applied load until failure and is responsible for the similar strength. Nevertheless the lam-

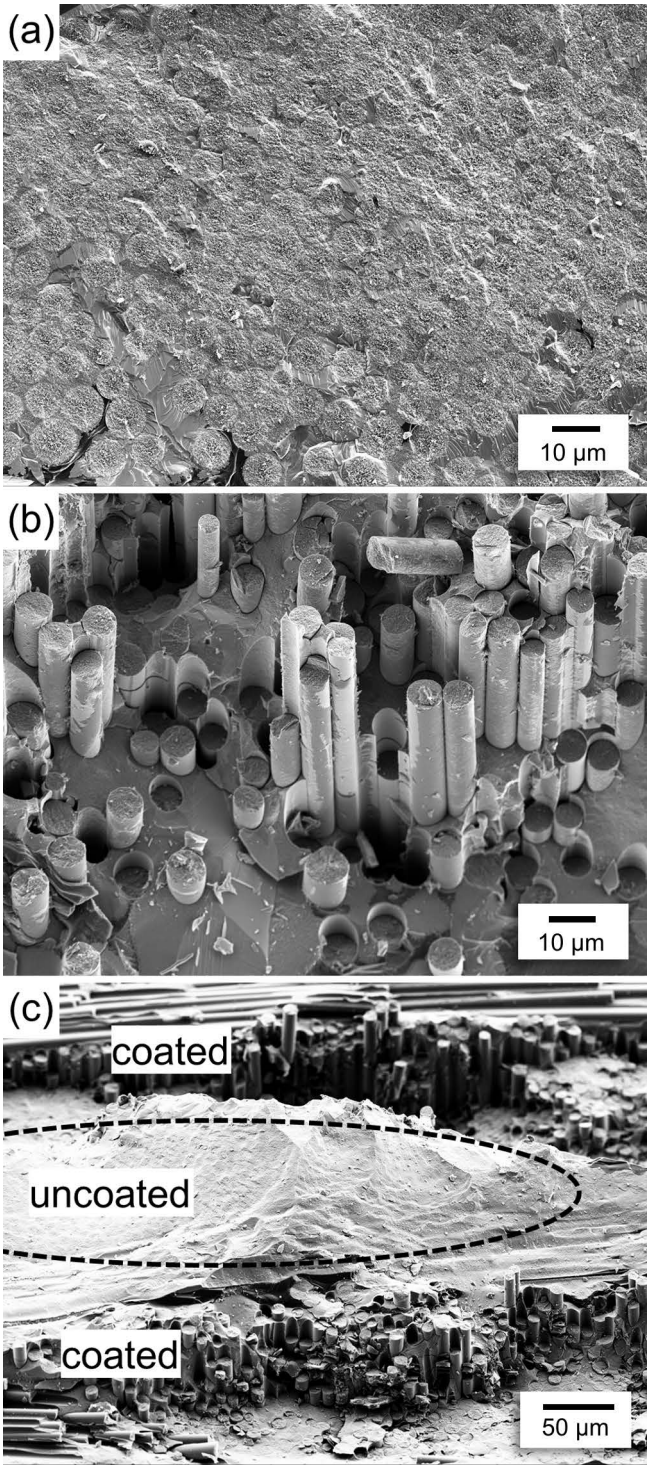

Fig. 10: SEM images of a fractured surface of the SiC/SiC laminate after 3PB test: (a) Fractured surface of the Type 3 composite; (b) Fractured surface of the Type 1 composite; (c) Fractured surface of the Type 2 composite showing two layers of coated SiC fabrics on the upper and lower side of the image and one layer of uncoated fabric in the middle.

inate was lacking the additional damage tolerance after the maximum stress had been reached. Presumably, after failure of the coated outer layer the propagating cracks could not be stopped owing to the high number of brittle layers. The composite without fiber coating (Type 3) showed very brittle behavior with an average strength of 103 ± 27 MPa. The Young's moduli of the three composites were similar but showed a strong deviation, ranging from 225 ± 57 GPa for the Type 3 composite, 240 ± 48 GPa for the Type 2 composite and 247 ± 72 GPa for the Type 1 composite. Although the span to thickness ratio of 10 was rather low, the bending tests show the functionality of the concept. In order to confirm these results, fractured surfaces were investigated by means of SEM. Without fiber coating, the surface was rather smooth (Fig. 10a). Energy-dissipating effects such as fiber pullout were not observed. The fibers remained intact after the reactive melt infiltration but were cramped into the strong matrix, which resulted in brittle behavior. In contrast, the composite with the three-layered fiber coating provided a moderate interface. The Si-BN layer effectuated the favorable fiber pullout and thereby an increase in strength and toughness was reached (Fig. 10b). The Type 2 composite showed both types of crack patterns (Fig. 10c). As observed, the crack deflection and fiber pullout occurred at the fiber/Si-BN interface as well as at the Si-BN/SiC interface.

IV. Conclusions

Damage-tolerant SiC/SiC composites were manufactured by means of reactive melt infiltration utilizing two- and three-layered fiber coatings on Tyranno SA3 fibers. The CVD coating consisted of a silicon-doped boron nitride, silicon carbide and, as the third layer, pyrolytic carbon. This complex fiber coating fulfilled a series of functions. The Si-BN provided a weak interface, which leads to an improvement of strength and strain in comparison to uncoated fibers. The SiC interlayer acted as barrier against the reactive melt and the pyC outer layer promoted good wetting and bonding with the carbon precursor. It was shown that a simple pyC outer layer has a huge impact on the formation of porosity after pyrolysis. The pyC layer provided such a strong bond with the precursor that shrinkage during pyrolysis was compensated by the evolution of a foam-like carbon. Thereby, homogeneous infiltration and conversion with silicon could be achieved. With the lack of fibers outside of bundles the precursor could shrink unimpeded and showed lower porosity with smaller pores. As a result, some of these dense carbon blocks remained unreacted. TEM analysis has shown that the coating was applied homogeneously and survived the harsh reactive melt infiltration, yet provided a good infiltration. The use of a NaOH-free precursor prevented degradation of the Si-BN layer. Thus, a non-porous composite with an average bending strength of 202 MPa was achieved. A laminate consisting of coated and uncoated fibers was manufactured which exhibited similar strength and strain but lacked full damage tolerance compared to the fully coated variant. It was observed that the pullout occurred at the fiber/Si-BN as well as the Si-BN/SiC interface. In the future these two concepts will be upscaled to more representative long bending samples as well as for tensile tests.

Acknowledgements

The financial support for the NewAccess project (03EK3544A) by the Germany's Federal Ministry of Education and Research (BMBF) and for the SiCaFis project (FR 1355/7 – 1) by the German Research Foundation (DFG) is gratefully acknowledged.

References

1 Gardiner, G.: Aeroengine composites, part 1: The CMC invasion. In: Composites World, August, Gardner Business Media Inc, Cincinnati, USA, 38 – 41, (2015).

2 Fitzer, E., Fritz, W., Gadow, R.: Development of silicon carbide composites, (in German), *Chem. Ing. Tech.*, **57**, 737 – 746, (1985).

3 Corman, G.S., Luthra, K.L.: Silicon melt infiltrated ceramic composites (HiPerComp™), In: Narottam P. Bansal: Handbook of ceramic composites. Kluwer Academic Publishers, 99 – 115, (2005).

4 Griesser, A., Pailler, R., Rebillat, F., Bruché, T., Bouillon, E., Philippe, E.: Enhanced SiC/SiC composites processed by reactive melt infiltration for high temperature applications, EC-CM15, Venice, Italy, 24 – 28 June 2012

5 Brennan, J.J.: Interfacial characterization of a slurry-cast melt-infiltrated SiC/SiC ceramic-matrix composite, *Acta Mater.*, **48**, 4619 – 4628, (2000).

6 Aoki, T., Ogasawara, T., Okubo, Y., Yoshida, K., Yano, T.: Fabrication and properties of Si-Hf alloy melt-infiltrated tyranno ZMI fiber/SiC-based matrix composites, *Composites: Part A*, **66**, 155 – 162, (2014).

7 Koch, D.: Microstructural modeling and thermomechanical properties, In: W. Krenkel: Ceramic matrix composites: Fiber reinforced ceramics and their applications. WILEY-VCH Verlag GmbH & Co.KGaA, 231 – 259, (2008).

8 He, M.Y., Hutchinson, J.W.: Kinking of a crack out of an interface, *J. Appl. Mech.*, **56**, 270 – 278, (1989).

9 Mukai, K., Yuan, Z.: Wettability of ceramics with molten silicon at temperatures ranging from 1693 to 1773 K, *Mater. Trans., JIM*, **41**, [2], 338 – 345, (2000).

10 Mainzer, B., Roder, K., Wöckel, L., Friess, M., Koch, D., Nestler, D., Wett, D., Podlesak, H., Wagner, G., Ebert, T., Spange, S.: Development of wound SiCBNx/SiNx/SiC with near stoichiometric SiC matrix via LSI process, *J. Eur. Ceram. Soc.*, **36**, 1571 – 1580, (2016).